NASA TECHNICAL MEMORANDUM

NASA TM X-71714

NASA TM X-71714

(NASA-TM-X-71714)   AERODYNAMIC DESIGN OF A   N75-24106
FREE POWER TURBINE FOR A 75 KW GAS TURBINE
AUTOMOTIVE ENGINE (NASA)   62 p HC $4.25
                              CSCL 21E   Unclas
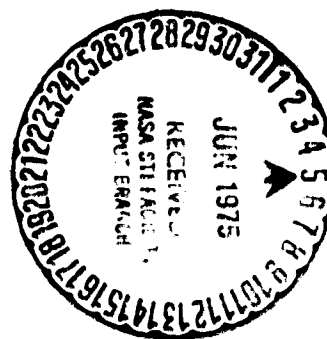   G3/44   21831

AERODYNAMIC DESIGN OF A FREE POWER TURBINE FOR A 75 KW GAS TURBINE AUTOMOTIVE ENGINE

by Milton G. Kofskey, Theodore Katsanis
Lewis Research Center
and Lawrence F. Schumann
U.S. Army Air Mobility R&D Laboratory
Cleveland, Ohio 44135
April, 1975

ABSTRACT

A single stage axial-flow turbine having a tip diameter of 15.41-centimeters was designed. The design specifications are given and the aerodynamic design procedure is described. The design includes the transition duct and the turbine exit diffuser. The aerodynamic information includes typical results of a parametric study, velocity diagrams, blade surface and wall velocities, and blade profile and wall coordinates.

AERODYNAMIC DESIGN OF A FREE POWER TURBINE FOR

A 75 KW GAS TURBINE AUTOMOTIVE ENGINE

by Milton G. Kofskey, Theodore Katsanis
and Lawrence F. Schumann

Lewis Research Center

SUMMARY

The Energy Research and Development Agency (ERDA) is conducting a program to demonstrate a gas turbine powered automobile that meets the 1978 Federal Emissions Standards with acceleration characteristics and fuel economy that are competitive with current conventionally powered vehicles. One part of the program consists of designing a new smaller engine which will meet the objectives of the program with a significant improvement in fuel economy over that obtained by the existing sixth generation engine and current vehicle manufactured by Chrysler Corporation. The improved fuel economy will result from increased turbine inlet temperature, reduced vehicle size, reduced unaugmented power to weight ratio, and possible improvements in the turbomachinery. The approach used in the design of the free power turbine for the new engine as well as the aerodynamic design parameters of the turbine are presented herein.

The free power turbine is a single stage axial flow design having a tip diameter of 15.41-cm. The turbine was designed for a rotative speed of 46,150 rpm; a hub to tip radius ratio of 0.78. A total efficiency of 0.85 was chosen for the design point. Losses due to low aspect ratio, rotor blade tip clearance, stator blade end clearance leakage and possible nonuniform inlet conditions were also taken into consideration in the determination of the design total efficiency. The turbine was designed for a work factor of 1.247 which reflects a

conservative design with high efficiency potential.

The transition duct and the turbine exit diffuser were designed to each have an optimum area ratio based on empirical studies.

INTRODUCTION

The Energy Research and Development Agency (ERDA) is conducting a program to demonstrate a gas turbine powered automobile that meets the 1978 Federal Emissions Standards with acceleration characteristics and fuel economy that are competitive with current conventionally powered vehicles. One part of this program involves an evaluation of an existing sixth generation engine and a current vehicle manufactured by the Chrysler Corporation. Another part of the program consists of designing a new engine to meet the objectives of the program with a significant improvement in fuel economy.

The existing or "baseline" engine delivers 112 KW in a 2000 Kg vehicle. The new or "upgraded" engine will deliver 75 KW in a 1600 Kg vehicle. The engine will have the capability for power augmentation to 90 KW through the use of variable guide vanes and water injection at the compressor inlet. Improved fuel economy will result from increased turbine inlet temperature, reduced vehicle size, reduced unaugmented power to weight ratio, and possible improvements in component efficiencies. The aerodynamic components for the "upgraded" engine have been designed at the Lewis Research Center. These include the compressor (ref. 1), the compressor-drive turbine (ref. 2), the free power turbine, the duct between the turbines, and the power turbine exit diffuser.

This report describes the design of the power turbine, the duct between the turbines, and the power turbine exit diffuser. The initial approach in the turbine design consisted of a parametric study to determine optimum turbine parameters such as work factor, size, and rotative speed. Vehicle, engine, and other restraints were considered in the final selection of these parameters. Upon completion of the parametric study, velocity diagrams, blade shapes, and surface velocities were obtained. The aerodynamic design parameters for the stator and rotor are given. Results of the duct and turbine exit diffuser design are shown in terms of velocity and pressure distributions.

SYMBOLS

$\mathcal{R}$	blade aspect ratio, b/c
b	blade height, cm
c	blade chord, cm
D_p	pressure-surface diffusion parameters, blade inlet relative velocity minus minimum blade surface relative velocity divided by blade inlet relative velocity
D_s	suction-surface diffusion parameters, maximum blade surface relative velocity minus blade outlet relative velocity divided by maximum blade surface relative velocity
D_{tot}	sum of suction- and pressure-surface diffusion parameter, $D_p + D_s$
Δh	specific work, J/g
m	meridional streamline distance, mm
p	pressure, newtons/cm^2
r	radius, cm
R	gas constant, J/(kg)(K)
R_x	reaction, blade outlet relative gas velocity squared minus blade inlet relative gas velocity squared divided by the blade outlet relative gas velocity squared
S	blade spacing or pitch, cm
T	temperature, K
U	blade velocity, m/sec
V	absolute gas velocity, m/sec
W	relative gas velocity, m/sec
Z	axial coordinate, mm
α	absolute gas flow angle as measured from meridional plane, deg

β relative gas flow angle as measured from meridional plane, deg

γ ratio of specific heats

θ relative angular coordinate, deg

ρ density, kg/m^3

σ solidity, c/s

ψ_z Zweifel loading coefficient,

Subscripts:

cr   conditions corresponding to Mach 1

e   exit

h   inner wall

i   inlet

m   mean

p   pressure surface

s   suction surface

sh   outer shroud

u   tangential component

x   axial component

1   station at stator inlet

2   station at rotor exit

Superscripts:

'   absolute total state

"   relative total state

TURBINE DESIGN

Parametric Study

The design parameters and turbine geometry were determined by an
iterative process wherein engine cycle calculations using estimated
component efficiencies and other engine losses were used to obtain a
first approximation of component mass flow, specific work output and
state conditions through the engine flow path. A parametric study
was made involving a range of overall turbine geometry, rotative
speed and work factor. Restraints imposed by engine, vehicle, trans-
mission and engine controls were taken into consideration for the
selection of the power turbine configuration. The design point efficiency for
this turbine was then used in the final engine cycle calculation for
determination of the design parameters which are tabulated in Table I.

The parametric study was made using Glassman's computer program
for preliminary design analysis of axial-flow turbines (reference 3).
The computations are based on mean-diameter flow properties and do
not consider any radial gradients. The output includes inlet and exit
annulus dimensions, turbine exit temperature and pressure, total and
static efficiencies, stator and rotor flow angles, and last stage
critical velocity ratios. The program was run over a range of work
factors from 1 to 2 and a range of turbine hub to tip radius ratios
from 0.6 to 0.9. Figures 1 thru 3 show typical plots used in the
parametric study. The figures show the variation of turbine parameters
with hub to tip radius ratio for rotative speeds of 40,000, 45,000, and
50,000 revolutions per minute. The tip clearance loss was based on a

tip clearance of 0.051 cm. The turbine size and rotative speed were selected from the following considerations:

1. The ratio of power turbine annulus area to compressor-drive turbine annulus area was selected to be approximately 2.0. This selection was based on annular diffuser studies for turbomachinery applications by Sovron and Klomp in reference 4. This reference indicated that this was the optimum area ratio with respect to pressure recovery for the given ratio of duct length to inlet passage height.

2. The design free stream stator hub exit flow angle was limited to a maximum value of 70 degrees from axial. This limitation was imposed for two reasons. First, operation at part power will result in the power turbine stator being closed by 4 to 5 degrees. Small errors in blade setting angles at angles greater than 75 degrees can result in a significant variation in stator throat area. Large variations in stator throat area in turn can result in large changes in compressor turbine inlet temperature. This is the result of the type of engine controls used. Also, as the stator exit flow angle approaches values of 80 degrees or more, blade trailing-edge blockage and associated losses become large. Since at part power operation where the stator exit flow angle is increased, this limit assures that blade trailing edge losses do not become excessive. It should be noted this limit also results in an increase in the turbine exit kinetic energy level.

3. The vehicle road load curve with a constant gear ratio between the power turbine and vehicle wheels must intersect the engine

power curve for 100% gas generator rotative speed at approximately 30% above the power turbine design speed. Further, the limiting stress must occur at a speed above the intersection point. This specification assures that power turbine will not be oversped to destruction during normal operating. This is illustrated by figure 4 which is a nondimensional plot of engine and vehicle road load horsepower as a function of power turbine rotative speed. The engine horsepower curve is for gas generator operation at design speed. The vehicle road load curve in the figure intersects the engine power curve at approximately 130 percent of design speed. The stress limit occurs at a speed slightly above 130% speed.

4. Only single stage axial flow turbines were considered because of cost considerations.

5. Zero rotor exit swirl was selected for two reasons. First, zero exit swirl or axial flow would provide better inlet flow conditions to the turbine exit diffuser and second, it minimizes the rotor exit kinetic energy and therefore minimizes the diffusion required by the exit diffuser.

Using the results of the parametric study and the above described constraints, a design rotative speed of 46,150 rpm, a hub to tip radius ratio of 0.78, and a rotor tip diameter of 15.41 centimeters was selected. A final value of the ratio of power turbine annulus area to compressor-drive turbine annulus area of 2.1 was selected.

A cross-sectional view of the compressor-drive turbine, transition duct, power turbine, and the exit diffuser is shown in figure 5. The power turbine incorporates a variable stator design to provide for

engine control and engine braking. Concentric spherical stator end walls are used to give a constant stator blade end clearance over the full range of stator settings. The figure also shows that rotor tip clearance is obtained by a recess in the casing over the rotor. In addition the rotor blade tip was designed to extend 0.010 centimeters into the recess. This type configuration was found to result in minimum tip clearance losses for an unshrouded rotor as reported in reference 5. A rotor tip clearance of 0.051 centimeters was chosen as the minimum value for hot operation.

The design requirements for the 15.41-centimeter tip diameter turbine are given in Table I. A work factor of 1.247 indicates a conservative design with high aerodynamic efficiency potential.

A total efficiency of 0.85 was selected as being achievable for this configuration. Losses due to low aspect ratio, rotor tip clearance, stator blade end clearance leakage and possible nonuniform inlet conditions, among others, were inputs in the selection of the design total efficiency.

Velocity Diagrams

The free-stream velocity diagrams were computed to meet the design requirements and are based on free vortex flow. The free-stream velocity diagrams and station nomenclature are shown in figure 6. The moderate amount of turning and the magnitude and increase in velocities throughout the turbine indicate a conservative design. The turning at the mean diameter is 35.2 degrees in the stator and 80.7 degrees in the rotor. All free-stream velocities are subsonic and there is an increase in relative velocity across all rotor blade sections indicating positive

reaction (R_x). Values of the stator and rotor reaction are shown in Tables II and III, respectively, along with the other aerodynamic parameters. Rotor or stage reaction can also be defined as the change in rotor relative kinetic energy divided by the turbine specific work ($w^2/2\Delta h$). Using this definition stage reactions of 0.245, 0.434, and 0.563 are obtained for the hub, mean, and tip sections respectively.

Table IV lists the design operating conditions of the stator and rotor based on equivalent conditions. The equivalent conditions into the stator were 10.13 N/cm^2 and 288.2°K. The stator inlet conditions of velocity, pressure, and flow angle were obtained from the results of the transition duct design.

STATOR DESIGN

A variable stator was designed to provide engine braking and control. Since this requires rotation through large arcs, the stator was designed with concentric spherical end walls. This design results in constant hub and shroud clearances for all stator blade settings and also simplifies the transition duct design. The pivot axis of the variable stator was chosen to lie on a radial line passing through the center of the concentric spheres (figure 5). This allows rotation through the entire operating range of the stator with no change in clearance.

The number of blades was chosen to be 23. A larger number would be desirable to reduce blade loading and to allow for a shorter chord to be chosen. However, the number was limited by the space requirement of the gear sector of the variable stator actuating mechanism on each blade shank.

The axial solidities for the hub, mean, and tip sections were determined from the loading criterion of reference 6. A value of 0.8 was selected for the Zweifel loading coefficient (ψ_2) since this value results in minimum losses assuming zero blade end clearances. The axial chords were determined from the calculated solidities and the known pitch. Since the blades are located between spherical walls and must be rotated through large arcs, thermal distortion may cause the blades to bind against the spherical walls. To minimize this possibility and to keep clearance losses low, the true chord was kept as short as possible. The blade chords (c), solidities (σ), and Zweifel loading coefficients (ψ_2) for the hub, mean, and tip sections are shown in Table II.

The blade profiles were obtained by first selecting the blade leading and trailing edge radii. Since the inlet Mach number was low, relatively large leading edge radii were used to minimize the effect of the variation of incidence. The smallest trailing edge radii consistent with fabrication considerations were selected. The values of the leading and trailing edge radii are given in Table II.

The blade mean camber line curvatures were determined by iteration to achieve the desired blade loading characteristics. The blade mean camber angle at the trailing edge was determined from the exit free-stream angle using a correction for blade blockage. The exit free-stream angle was obtained from the design velocity diagram.

Estimates of the free-stream angle at stator inlet for both the design and the off-design (50% compressor-drive turbine speed, 75% stator throat area) cases were obtained from runs of the computer program MERIDL (reference 7) for the transition duct. Using these estimated free-stream angles and the loss correlations of references 8 and 9, it was determined that the stator would operate in the region of minimum incidence losses over the entire engine operating range if it were designed for -9° incidence.

Using the free-stream angles obtained from the MERIDL run for the transition duct at design conditions and the design incidence angle of -9°, the blade mean camber angle at the leading edge was determined. The flow through the stator blade rows was then analyzed using MERIDL, which calculates the hub to shroud velocity profile at the mid-channel, the incidence and deviation angles, and the necessary input for the TSONIC program (reference 10), to obtain a finite difference blade to blade solution.

After satisfactory blade loadings were obtained with MERIDL, TSONIC was used to obtain the final blade surface velocities for the hub, mean, and tip sections. The results are shown in figure 7. The figure shows loading and diffusion characteristics obtained. The blade coordinates were also obtained from TSONIC and are shown in Table V.

MERIDL was then run for the off-design case as defined earlier in this section to check incidence angles. The free-stream conditions at the inlet were obtained from a MERIDL run for the transition duct for this off-design case. The incidence angles were found to be approximately 0° from hub to tip which were considered satisfactory. The incidence angles for the design and the off-design cases as calculated by MERIDL are shown in Table VI. The blade profiles and flow passages for the stator and rotor are shown in figure 8.

ROTOR DESIGN

The chord length of the mean section of the rotor was selected using
the blade height determined during PRELIMINARY DESIGN and a selected
value of aspect ratio of 1.3. This value is in the range where losses
associated with low aspect ratios are not significant (reference 11).
The number of blades was then determined for optimum solidity assuming
a Zweifel loading coefficient (ψ_z) of 0.8 (reference 6). This optimum
solidity criterion was then used to determine the chord lengths of the
hub and tip. The aerodynamic parameters for the rotor blades are shown
in Table III.

The rotor blade profiles were determined in much the same way as
the stator blade profiles. The inlet and exit free stream angles were
obtained from the design velocity diagram. The exit mean camber angle
was determined from the exit free stream angle using a correction for
blade blockage. Based on the loss correlations of reference 9, the
inlet mean camber angle was designed for negative incidence of 7 degrees
to minimize the amount of positive incidence and hence the losses that
would occur for the off-design case previously specified in the STATOR
DESIGN section. The design incidence angles are shown in Table VI.

The computer program TSONIC was used to obtain the surface veloc-
ities and blade coordinates. Plots of the surface velocities are
shown in figure 9. The figure shows that the velocities are subsonic
everywhere and that there is very little diffusion on the blade sur-
faces. The computer program of reference 12 was used to convert the
coordinates obtained from TSONIC to the generally accepted format for
fabrication. These coordinates are shown in Table VII.

TRANSITION DUCT

The transition duct carries flow from the compressor turbine exit to the inlet of the power turbine stator. The transition duct area ratio of 2.1 was chosen as explained in the PRELIMINARY DESIGN section. The length of the transition duct is limited by overall engine length constraints. The transition duct shape is then determined primarily by the requirement to blend smoothly between the compressor turbine rotor outlet, and the concentric spherical endwall surfaces for the power turbine stator. A further requirement for efficient diffusion is that there be a smoothly increasing area variation through the duct with a minimum peak curvature.

The curve used for the duct walls is a mathematical spline fit curve (ref. 13). Using a mathematically defined curve enables a precise specification of as many coordinates as desired. Flow analysis programs used for this analysis (ref. 7) use the mathematical spline fit curve. Figure 10 shows the transition duct, and Table VIII contains the hub and shroud coordinates at 2 mm axial increments.

The transition duct flow was analyzed with an inviscid flow analysis. The purpose of this analysis is to assure that there are no unnecessary velocity peaks followed by excessive adverse pressure gradients. There are three support struts, as shown in figure 4. They are streamlined and will be aligned with the flow angle at 50% gas generator speed. The struts block approximately 2% of the flow area and were neglected for the inviscid flow analysis. The inviscid analysis was done with the MERIDL program (ref. 7). The mass flow, temperature, pressure and whirl angle are shown in Table IX. The

results of this analysis are shown in figure 11. This figure shows hub
and shroud pressure and velocity distributions for both the design
point and 50% compressor-drive turbine speed.

Boundary layer analysis was not helpful because of the strong inter-
action between the boundary layer and the free stream. Therefore, the
basic transition duct design is based on the overall area ratio. The
area ratio chosen is near the optimum indicated by the experimental
work of Sovran & Klomp (ref. 4) as discussed in PRELIMINARY DESIGN.

Since the transition duct analysis is inviscid, the angular momen-
tion at the leading edge of the power turbine stator is assumed to be
the same as that at the exit of the compressor-drive turbine rotor.
The through flow component of flow is determined by the mass flow and
by the equilibrium equation assuming a 2% loss of total pressure.
The resulting angles are calculated by the MERIDL program (ref. 7),
and are shown in figure 12 for the design point and 50% compressor-
drive turbine speed.

DIFFUSER DUCT DESIGN

The area ratio for the diffuser duct was determined from the work of Sovran & Klomp (ref. 4). The mean channel length, $\overline{L}$, is approximately 7.61 cm and the radial height, Δr, at the entrance of the diffuser is 1.77 cm so that $\overline{L}/\Delta r$ (see figure 17 of ref. 4) is 4.3. For this value of $\overline{L}/\Delta r$ this figure shows the optimum area ratio is 1.9. The static pressure recovery from this figure should be about 58% of the dynamic head.

The overall turbine design requires a radial diffuser outlet. The area ratio of 1.9 determines the axial width of 2.06 cm at the outlet of the diffuser ($r_o = 11.25$ cm). For optimum diffusion it is necessary to have a smooth area variation with smoothly varying curvature. The curve that was used is one with sinusoidally varying curvature; that is, the curve satisfies the equation

$$\frac{d\alpha_m}{ds} = \frac{\pi^2}{4S} \, \text{Sin}\left(\frac{\pi s}{S}\right) \tag{1}$$

where

$\dfrac{d\alpha_m}{ds}$	is the wall curvature
s	is the distance along the wall
S	is the overall length of the wall
α_m	is the angle from axial

The actual coordinates of both hub and shroud were obtained by the numerical solution of eq. (1). The constant $\pi^2/4S$ in equation (1) was determined so that the change in α_m would be 90°.

Figure 13 shows the resulting diffuser shape, and Table X gives
the tabulated coordinates. The diffuser duct was analyzed with the
MERIDL program (ref. 7). The design flow conditions (mass, tempe.a-
ture and pressure) are shown in Table XI. Figure 14 shows the hub
and shroud pressure and velocity distributions.

REFERENCES

1. Galvas, Michael R.: Compressor Design for the Energy Research
   and Development Agency (ERDA) Automotive Gas Turbine Program.
   NASA X-71719, 1975.

2. Roelke, Richard J.; and McLallin, Kerry L.: The Aerodynamic Design
   of a Compressor-Drive Turbine for Use in a 75 kW Automotive Engine.
   NASA TM X-71717, 1975.

3. Glassman, Arthur J.: Computer Program for Preliminary Design Analysis
   of Axial-Flow Turbines. NASA TN D-6702, 1972.

4. Sovran, Gino; and Klomp, Edward D.: Experimentally Determined Optimum
   Geometries for Rectilinear Diffusers with Rectangular, Conical or
   Annular Cross Section. Fluid Mechanics of Internal Flow, Gino
   Sovran ed., Elsevier Publishing Co., 1967, pp. 270-312.

5. Kofskey, Milton G.: Experimental Investigation of Three Tip-
   Clearance Configurations over a Range of Tip Clearance Using a
   Single-Stage Turbine of High Hub- to Tip-Radius Ratio. NASA TM X-
   472, 1961.

6. Miser, James W.; Stewart, Warner L.; and Whitney, Warren J.: Analysis
   of Turbomachine Viscous Losses Affected by Changes in Blade Geom-
   etry. NACA RM E56F21, 1956.

7. Katsanis, Theodore; and McNally, William D.: Fortran Program for
   Calculating Velocities and Streamlines on the Hub-Shroud Mid-Channel
   Flow Surface of an Axial or Mixed-Flow Turbomachine. I - User's
   Manual. NASA TN D-7343, 1973.

8. Ainley, D. G.; and Mathieson, G. C. R.: An Examination of the Flow and Pressure Losses in Blade Rows of Axial-Flow Turbines. Rept. No. R86, National Gas Turbine Establishment, 1951.

9. Glassman, Arthur J., ed.: Turbine Design and Application. NASA SP-290-VOL-II, 1973.

10. Katsanis, Theodore: Fortran Program for Calculating Transonic Velocities on a Blade-to-Blade Stream Surface of a Turbomachine. NASA TN D-5427, 1969.

11. Kofskey, Milton G.; and Nusbaum, William J.: Design and Cold-Air Investigation of a Turbine for a Small Low-Cost Turbofan Engine. NASA TN D-6967, 1972.

12. Katsanis, Theodore: Fortran Program for Calculating Axial Turbo-machinery Blade Coordinates. NASA TM X-2061, 1970.

13. Katsanis, Theodore: Fortran Program for Spline Fit Curve. NASA TM X-1707, 1968.

TABLE I. - DESIGN OPERATING VALUES

	Engine operation	Equivalent condition
Inlet total temperature, T', K	1154	288.2
Inlet total pressure, p', N/cm^2	19.55	10.13
Mass flow, kg/sec	0.590	0.624
Specific work, Δh, J/g	137.1	35.1
Turbine rotative speed, rpm	46150	23343
Rotor blade speed (mean section), U_m, m/sec	331.4	167.6
Work factor $\Delta h \times 10^3 / U_m^2$	1.247	1.247
Total-to-total pressure ratio, p'_1/p'_2	1.678	1.712
Total efficiency	0.850	.850
Static efficiency	0.741	.741

TABLE II. - STATOR AERODYNAMIC PARAMETERS

| | Chord (cm) | L.E.R. (cm) | T.E.R. (cm) | Diffusion[a] | | | Solidity σ | Reaction[a] Rx | Aspect ratio[b] AR | Zweifel loading coefficient, ψ_z |
				D_s	D_p	D_{tot}				
Hub	1.900	0.076	0.025	0.15i	0.270	0.421	1.16	0.883	-----	0.798
Mean	2.151	0.089	0.030	0.132	0.242	0.374	1.15	0.857	0.789	0.764
Tip	2.403	0.102	0.036	0.107	0.218	0.325	1.14	0.845	-----	0.742

[a] See Symbol list
[b] Based on chord length at mean diameter

Blade height = 1.697 cm (rotor exit)

TABLE III. - ROTOR AERODYNAMIC PARAMETERS

| | Chord (cm) | L.E.R. (cm) | T.E.R. (cm) | Diffusion[a] | | | Solidity[a], σ | Reaction, Rx | Aspect ratio[b], $A\!R$ | Zweifel loading coefficient, ψ_z |
				D_p	D_s	D_{tot}				
Hub	1.463	0.048	0.031	0.355	0.106	0.461	2.053	0.505	----	0.840
Mean	1.311	0.038	0.025	0.323	0.159	0.482	1.613	0.771	1.29	0.819
Tip	1.278	0.029	0.019	0.232	0.093	0.325	1.399	0.823	----	0.768

[a]See Symbol list

[b]Based on chord length at mean diameter

Blade height = 1.697 cm

Tip clearance = 0.051 cm

TABLE IV. - TURBINE EQUIVALENT PARAMETERS

Stator exit & rotor inlet	Description	Hub	Mean	Tip
	P', N/cm^2	9.727	9.727	9.727
	P, N/cm^2	6.396	6.991	7.422
	T', K	288.2	288.2	288.2
	T, K	255.7	262.2	266.8
	T'', K	264.0	267.3	270.9
	V/V_{cr}	0.823	0.735	0.668
	V_u/V_{cr}	0.768	0.673	0.599
	V_x/V_{cr}	0.296	0.296	0.296
	α, deg	68.9	66.2	63.7
	W/W_{cr}	0.437	0.337	0.306
	W_u/W_{cr}	0.308	0.138	-0.008
	W_x/W_{cr}	0.309	0.307	0.305
	β, deg	44.9	24.2	-1.5
	U, m/sec	146.9	167.6	188.4
	U/V_{cr}	0.473	0.540	0.606
	V_{cr}, m/sec	310.6	310.6	310.6
	W_{cr}, m/sec	297.3	299.2	301.2
	p'', N/cm^2	6.852	7.472	7.841
	e', kg/m^3	1.176	1.176	1.176
	e, kg/m^3	0.872	0.929	0.969
	e'', kg/m^3	0.945	0.974	1.008

TABLE IV. - Concluded.

Rotor exit	Description	Hub	Mean	Tip
	P', N/cm^2	5.918	5.918	5.918
	P, N/cm^2	5.427	5.427	5.427
	T', K	253.3	253.3	253.3
	T, K	247.1	247.1	247.1
	U, m/sec	146.9	167.6	188.4
	U/V_{cr}	0.504	0.576	0.647
	V/V_{cr}	0.383	0.383	0.383
	V_u/V_{cr}	0	0	0
	V_x/V_{cr}	0.383	0.383	0.383
	α	0	0	0
	V_{cr}, m/sec	291.2	291.2	291.2
	W/W_{cr}	0.621	0.673	0.727
	W_u/W_{cr}	0.494	0.560	0.625
	W_x/W_{cr}	0.375	0.373	0.370
	β, deg	52.8	56.4	59.4
	ρ', kg/m^3	0.814	0.814	0.814
	ρ, kg/m^3	0.765	0.765	0.765
	ρ'', kg/m^3	0.849	0.875	0.906
	p'', N/cm^2	6.843	7.146	7.493
	r, cm	6.001	6.858	7.706

TABLE V. - STATOR BLADE SECTION COORDINATES
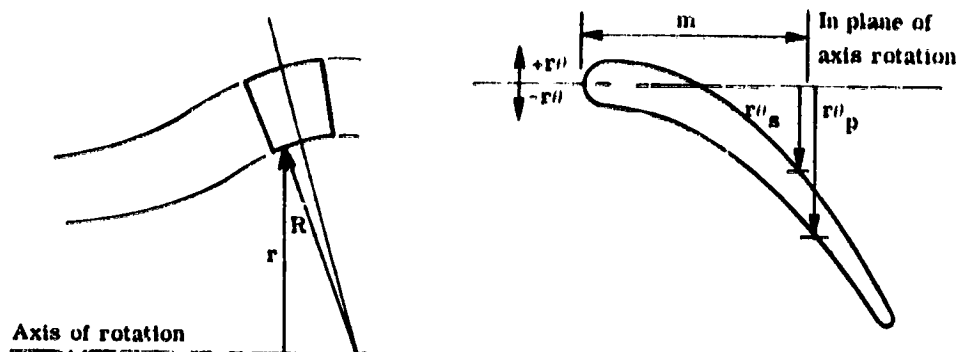
Hub				Mean				Tip			
Radius, R, mm											
60.10				68.58				77.06			
Leading-edge radius, mm											
0.76				0.89				1.02			
Trailing edge radius, mm											
0.25				0.30				0.36			
Blade stacking coordinates											
m	r	θ		m	r	θ		m	r	θ	
5.30	58.65	-4.04		6.17	66.43	-3.81		7.09	75.21	-3.64	
Blade coordinates											
m	r	θ_s	θ_p	m	r	θ_s	θ_p	m	r	θ_s	θ_p
0.	57.25	0.	0.	0.	65.33	0.	0.	0.	73.30	0.	0.
0.75	57.48	0.76	-0.85	0.86	65.79	0.78	-0 86	1.09	73.63	0.79	-.0
1.51	57.71	0.54	-1.29	1.72	66.32	0.57	-1.25	2.17	73.94	0.53	-1.5
2.26	57.94	0.22	-1.86	2.58	66.78	0.28	-1.73	3.26	74.22	0.19	-1.90
3.02	58.14	-0.20	-2.59	3.44	67.08	-0.09	-2.35	4.34	74.47	-0.28	-2.21
3.77	58.34	-0.76	-3.50	4.30	67.31	-0.60	-3.11	5.42	74.75	-0.93	-3.48
4.53	58.52	-1.50	-4.57	5.16	67.49	-1.27	-4.02	6.51	75.01	-1.77	-4.50
5.28	58.70	-2.48	-5.78	6.02	67.64	-2.12	-5.06	7.59	75.23	-2.81	-5.62
6.04	58.85	-3.73	-7.12	6.88	67.79	-3.19	-6.21	8.68	75.49	-4.04	-6.83
6.79	58.98	-5.21	-8.56	7.74	67.97	-4.46	-7.45	9.76	75.69	-5.44	-8.09
7.55	59.13	-6.91	-10.05	8.60	68.17	-5.89	-8.75	10.85	75.89	-6.96	-9.42
8.30	59.23	-8.77	-11.55	9.46	68.43	-7.45	-10.08	11.93	76.10	-8.59	-10.73
9.06	59.36	-10.77	-13.02	10.32	68.68	-9.10	-11.40	13.02	76.25	-10.27	-12.66
9.81	59.46	-12.83	-14.49	11.18	68.91	-10.81	-12.70	14.10	76.40	-11.99	-13.39
10.56	59.56	-14.92	-14.92	12.04	69.09	-12.53	-13.99	15.19	76.53	-13.78	-13.78
				12.90	69.14	-14.31	-14.31				

TABLE VI. - STATOR AND ROTOR INCIDENCE ANGLE

All angles are in deg
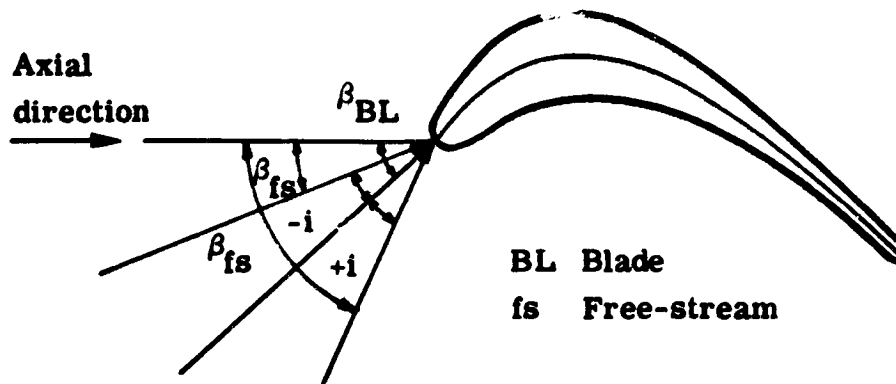
(a) Design case - 100% stator throat area,
100% gas generator speed, mass flow = 0.590 kg/sec

% distance hub to tip	Stator inlet		Rotor inlet	
	Blade angle, β_{BL}	Incidence, i	Blade angle, β_{BL}	Incidence, i
0	-22.5	-8.21	-50.0	-5.0
25	-22.3	-9.55		
50	-22.0	-9.45	-29.0	-4.8
75	-21.8	-9.45		
100	-21.5	-9.81	-7.0	-8.5

(b) Off-design case - 75% stator throat area,
50% gas generator speed,
mass flow = 0.203 kg/sec

% distance hub to tip	Stator inlet	
	Blade angle, β_{BL}	Incidence, i
0	-28.4	-0.01
25	-28.2	-0.32
50	-27.9	-0.10
75	-27.7	0.26
100	-27.4	0.29

TABLE VII. - ROTOR BLADE COORDINATES

[All coordinate dimensions are in mm].

53 Blades
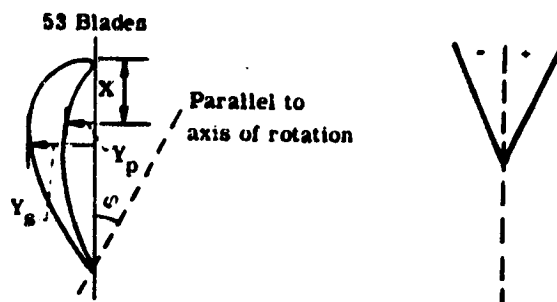
	Hub		Mean		Tip	
	Radius					
	60.10		68.58		77.06	
	Leading-edge radius					
	0.48		0.38		0.29	
	Trailing-edge radius					
	0.31		0.25		0.19	
	Orientation angle. φ. deg					
	-10.22		-25.00		-34.?1	
	Blade stacking coordinates (C G.)					
X	$\bar{Y}$	$\bar{X}$		Y	X	$\bar{Y}$
6.581	2.962	5.762		2.243	5 734	1.804

		Blade coordinates				
X	Y_p	Y_s	Y_p	Y_s	Y_p	Y_s
0.	.4792	.4792	3834	3834	.2875	.2875
.4792	0	1 453	.0115	1 215	.0728	.8722
.9585	.3412	2 183	4620	1.859	.4217	1.315
1.438	1.001	2.803	.9106	2.408	.7189	1.720
1.917	1.516	3.324	1.259	2.858	.9700	2.076
2.396	1.917	3.757	1.532	3.209	1.177	2.377
2.875	2.226	4.114	1.743	3.470	1.348	2.624
3.355	2.456	4.399	1.905	3.658	1.482	2.816
3.834	2.626	4.622	2.024	3.782	1.585	2.954
4.313	2.747	4.789	2.10.	3.853	1.658	3.046
4.792	2.829	4.900	2.157	3.876	1.704	3.092
5.272	2.879	4.965	2.176	3.861	1.725	3.098
5.751	2.902	4.984	2.168	3.807	1.725	3.067
6.230	2.902	4.965	2.136	3.721	1.702	3.000

TABLE VII. - Concluded

X	Y_L	Y_u	Y_L	Y_u	Y_L	Y_u
6.709	2.879	4.907	2.082	3.608	1.664	2.904
7.189	2.833	4.819	2.007	3.466	1.606	2.782
7.668	2.768	4.699	1.913	3.301	1.536	2.636
8.147	2.682	4.549	1.804	3.115	1.447	2.473
8.626	2.576	4.376	1.677	2.910	1.346	2.293
9.106	2.454	4.177	1.536	2.690	1.231	2.099
9.585	2.316	3.959	1.378	2.454	1.100	1.892
10.06	2.160	3.719	1.208	2.203	.9547	1.675
10.54	1.990	3.462	1.026	1.942	.7975	1.451
11.02	1.806	3.188	.8281	1.670	.6269	1.217
11.50	1.606	2.897	.6211	1.388	.4447	.9777
11.98	1.386	2.584	.4006	1.098	.2492	.7323
12.46	1.143	2.551	.1706	.8013	.0422	.4792
12.79					.1917	.1917
12.94	.8722	1.894	.0115	.4965		
13.11			.2492	.2492		
13.42	.5732	1.512				
13.90	.2396	1.106				
14.38	.0058	.6748				
14.63	.3067	.3067				

TABLE VIII

TRANSITION DUCT COORDINATES
(See Fig. 10)
Coord. in mm

z	r_h	r_{sh}
0	44.45	55.88
2	44.45	55.89
4	44.45	55.91
6	44.45	55.96
8	44.46	56.04
10	44.48	56.17
12	44.51	56.35
14	44.56	56.58
16	44.63	56.88
18	44.72	57.26
20	44.83	57.72
22	44.98	58.26
24	45.15	58.88
26	45.36	59.56
28	45.60	60.29
30	45.87	61.07
32	46.19	61.88
34	46.54	62.72
36	46.94	63.59
38	47.40	64.50
40	47.92	65.45
42	48.51	66.44
44	49.18	67.47
46	49.94	68.50
48	50.77	69.50
50	51.66	70.43
52	52.61	
54	53.58	
56	54.52	

TABLE IX

TRANSITION DUCT INLET CONDITIONS

	DESIGN PT.	50% SPEED
Mass Flow	.5897 Kg/sec	.2032 Kg/sec
T_h'	1156.2 K	1066.3 K
T_{mean}'	1150.2 K	1065.7 K
T_{sh}'	1146.2 K	1065.3 K
P_h'	20.3730 N/cm^2	12.0440 N/cm^2
P_{mean}'	20.4930 N/cm^2	12.0230 N/cm^2
P_{sh}'	20.5646 N/cm^2	12.0060 N/cm^2
α_h	21.9°	21.2°
α_{mean}	20.8°	19.2°
α_{sh}	19.5°	16.6°

$\gamma = 1.32$

$R = 287.053$ J/Kg-K

TABLE X

DIFFUSER DUCT COORDINATES
(See Fig. 13)
Coord. in mm

z_h	r_h	z_{sh}	r_{sh}
0.	60.10	0.	77.70
2.87	60.10	2.29	77.70
6.14	60.10	4.59	77.72
9.41	60.13	6.88	77.78
12.68	60.22	9.17	77.90
15.94	60.39	11.45	78.10
19.19	60.67	13.73	78.39
22.44	61.08	15.99	78.79
25.65	61.65	18.22	79.31
28.83	62.40	20.42	79.97
31.96	63.33	22.56	80.77
35.03	64.48	24.65	81.73
38.00	65.84	26.66	82.83
40.86	67.41	28.57	84.09
43.59	69.21	30.38	85.51
46.16	71.22	32.07	87.06
48.57	73.43	33.62	88.75
50.78	75.84	35.03	90.55
52.79	78.41	36.29	92.47
54.59	81.14	37.40	94.48
56.17	84.00	38.35	96.56
57.52	86.98	39.16	98.71
58.67	90.04	39.81	100.91
59.61	93.17	40.34	103.14
60.35	96.35	40.74	105.40
60.92	99.57	41.03	107.67
61.33	102.81	41.22	109.96
61.61	106.06	41.35	112.50
61.78	109.32		
61.86	112.50		

TABLE XI

DIFFUSER DUCT INLET CONDITIONS

Mass Flow	.590 Kg/sec
T'	1037.4 K
P'	11.6452 N/cm^2
γ	1.322
R	287.053 J/Kg-K

Figure 1. Variation of turbine parameters with hub-tip radius ratio for constant input.

Figure 4.— Engine and Road Load Power Matching Characteristics for a Constant Gear Ratio between Power Turbine and Vehicle Wheels

Support struts
3 reqd

Pivot axis

Diffuser

Transition duct

Compressor-drive Turbine   Power turbine

Figure 5- Schematic of turbine, transition duct, and diffuser components.

Figure 6.- Free-stream velocity diagrams.
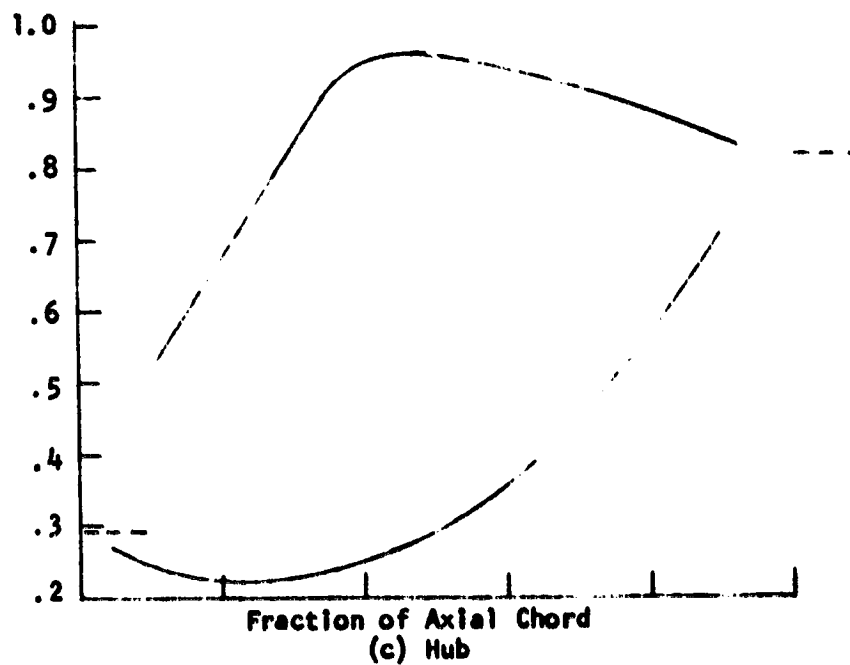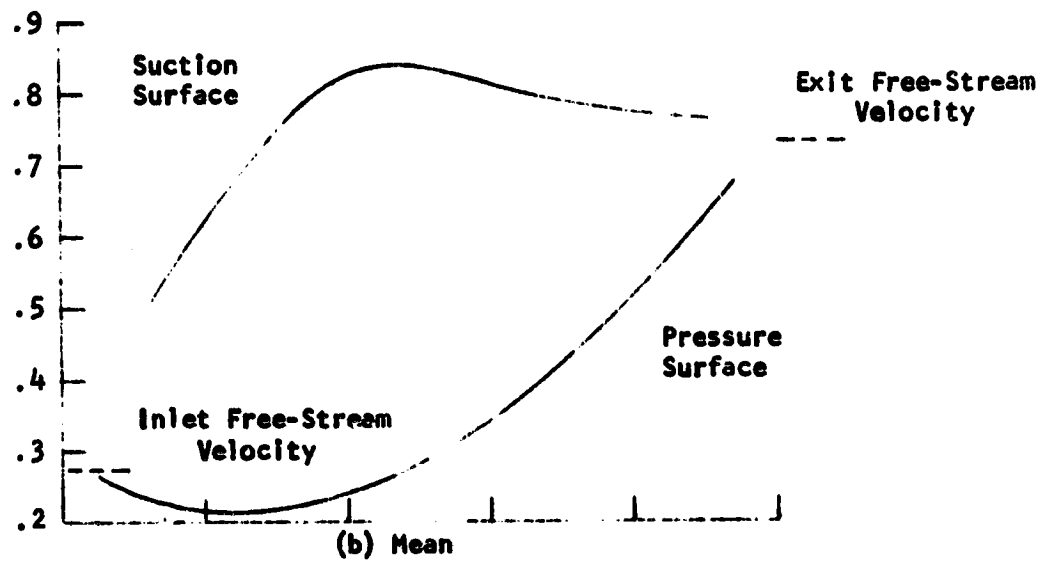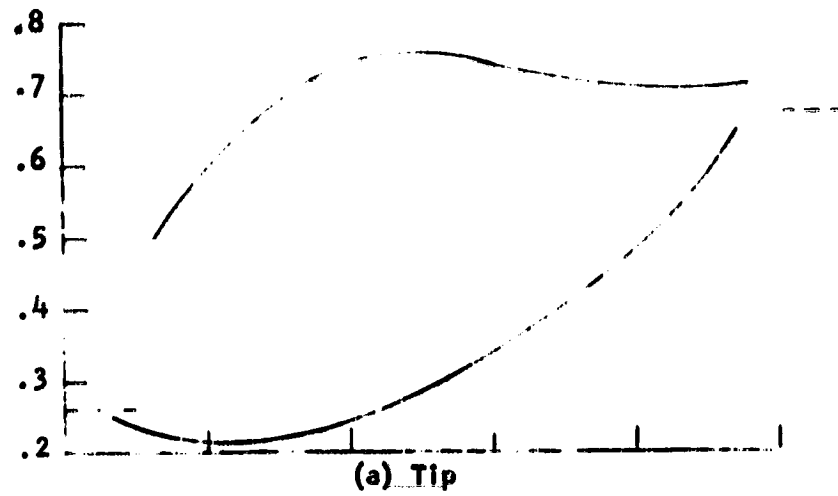
Figure 7 -- Design Stator Blade Surface Velocities

Figure 8 — Stator and Rotor Blade Passages and Profiles
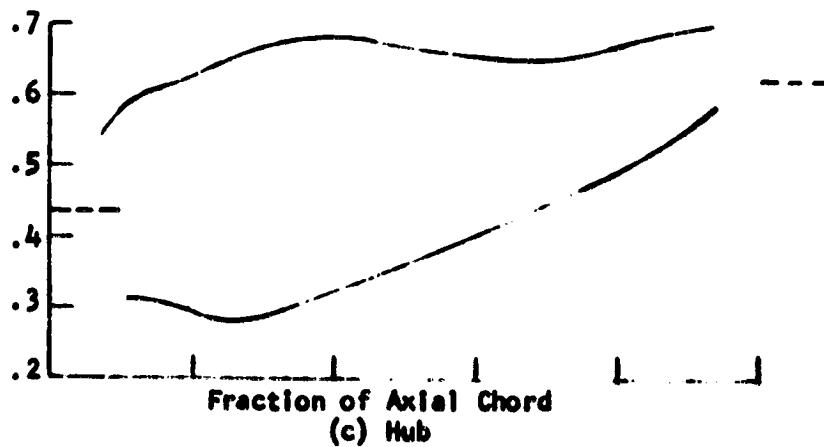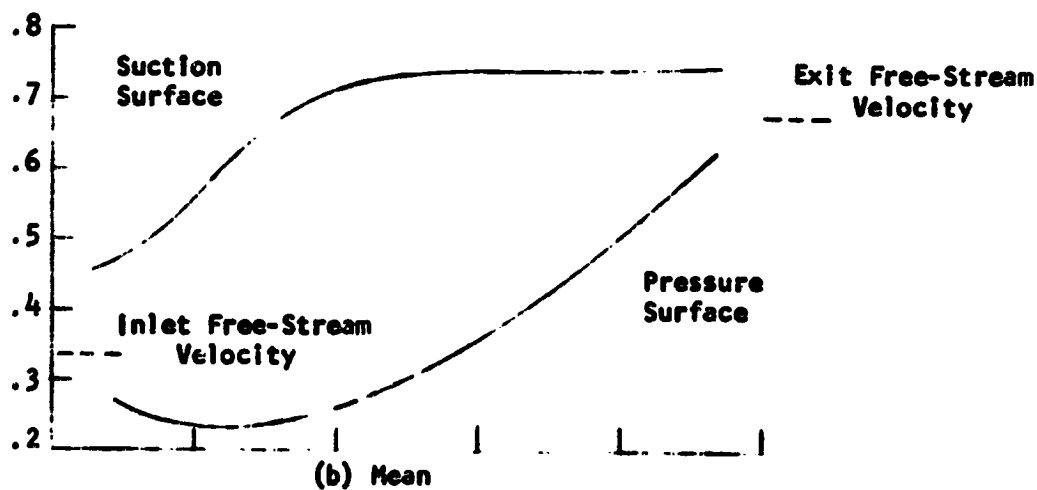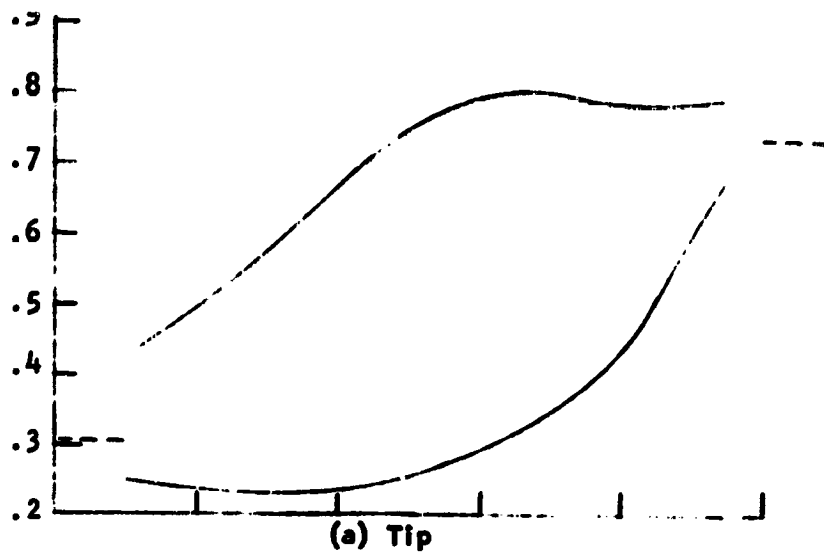
Figure 9 -- Design Rotor-Blade Surface Velocities

Figure 10.- Transition Duct

ORIGINAL PAGE IS
OF POOR QUALITY

APPROX SCALE 2:1
ALL DIMENSIONS
GIVEN IN mm.

77.06 RAD.

60.10 RAD.

10·3·74
T. Katsanis.

r₄

r (see Table XIII)

81.28

z (see Table XIII)

44.45 RAD.

55.88 RAD.
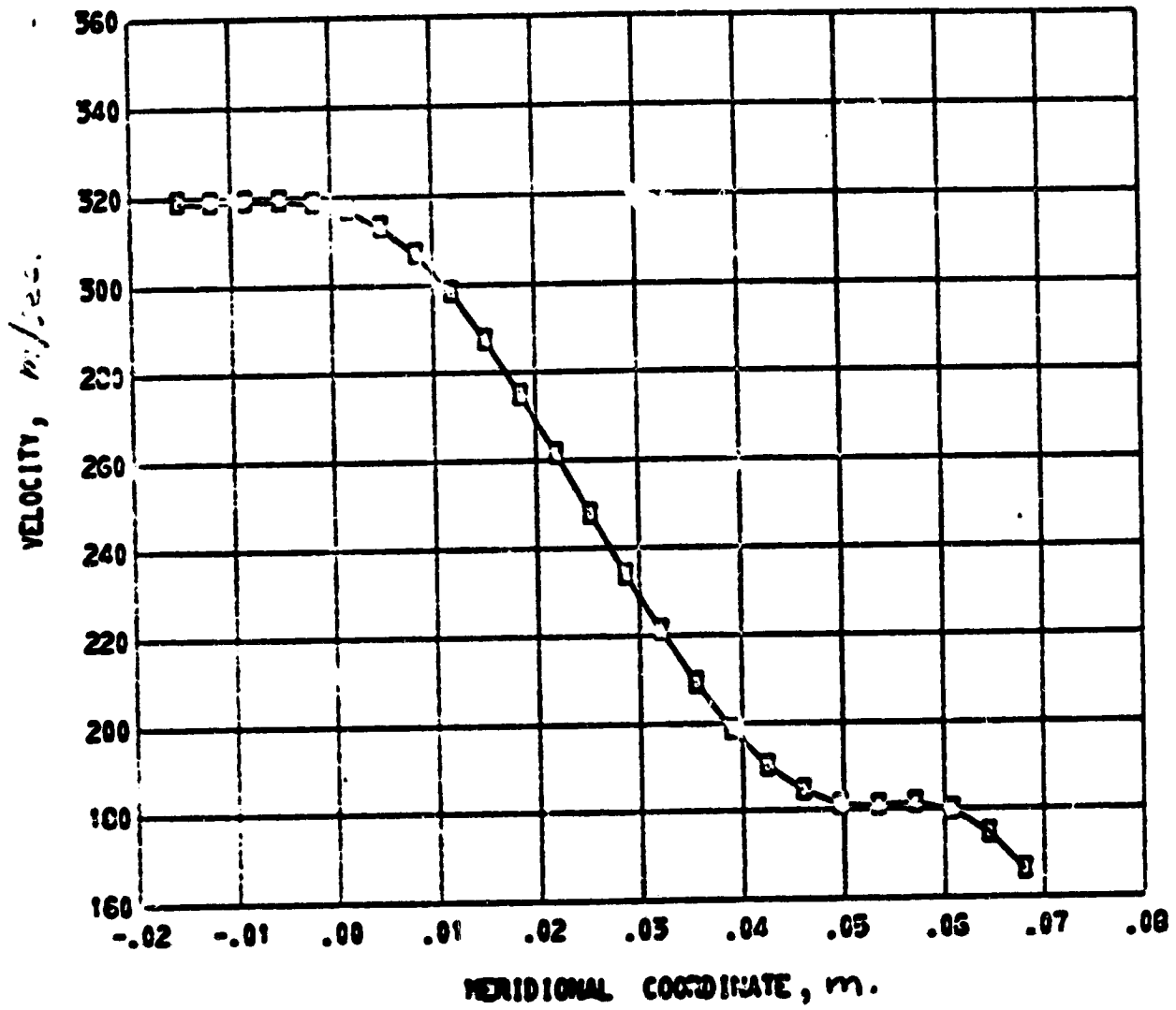
Figure 11. -- Interstage Transition Duct
a. Design Point Velocity Distribution - Hub
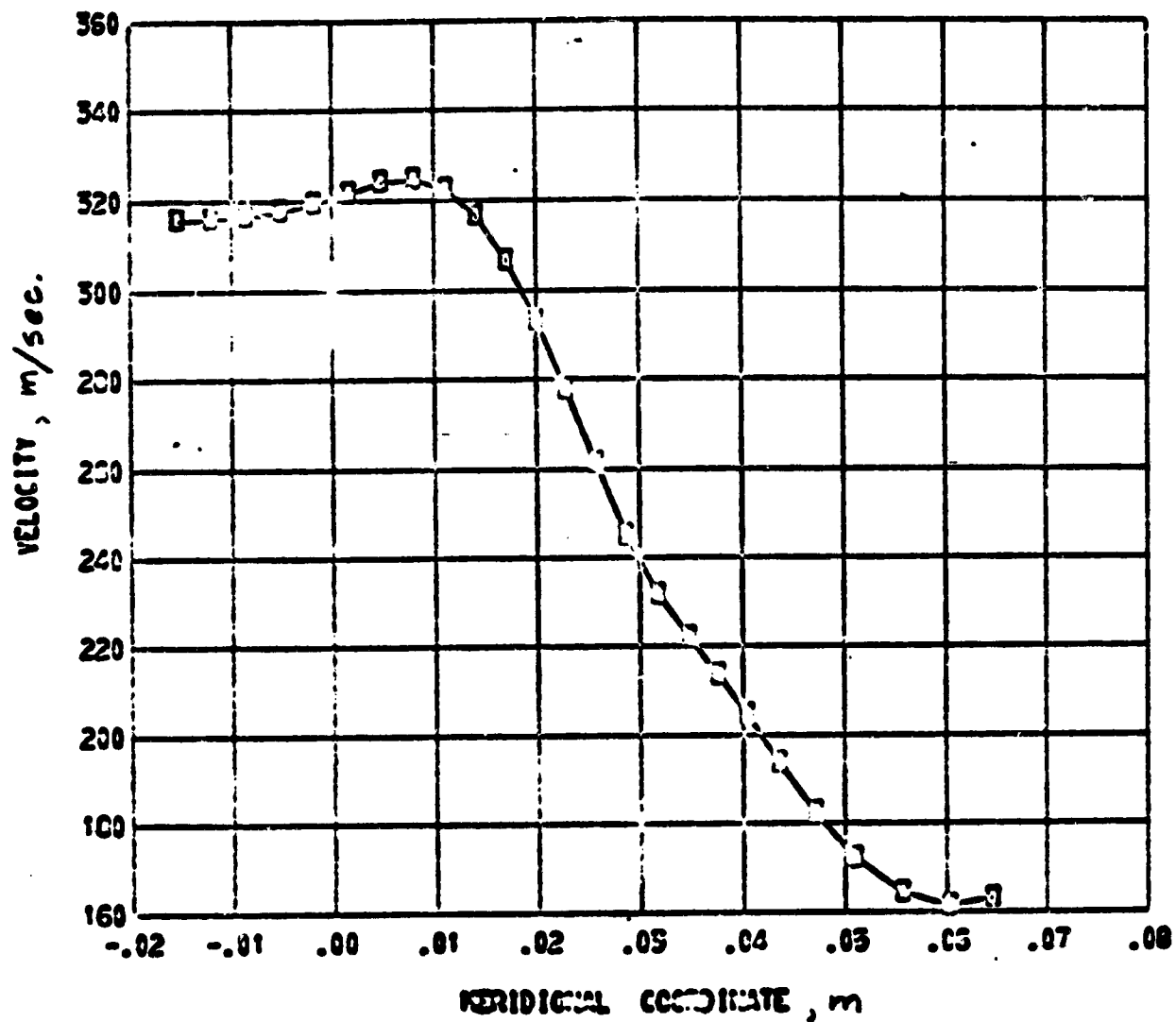
Figure II. -- Continued
b. Design Point Velocity Distribution - Shroud

STREAMLINE DISTANCE FROM UPSTREAM BOUNDARY, m
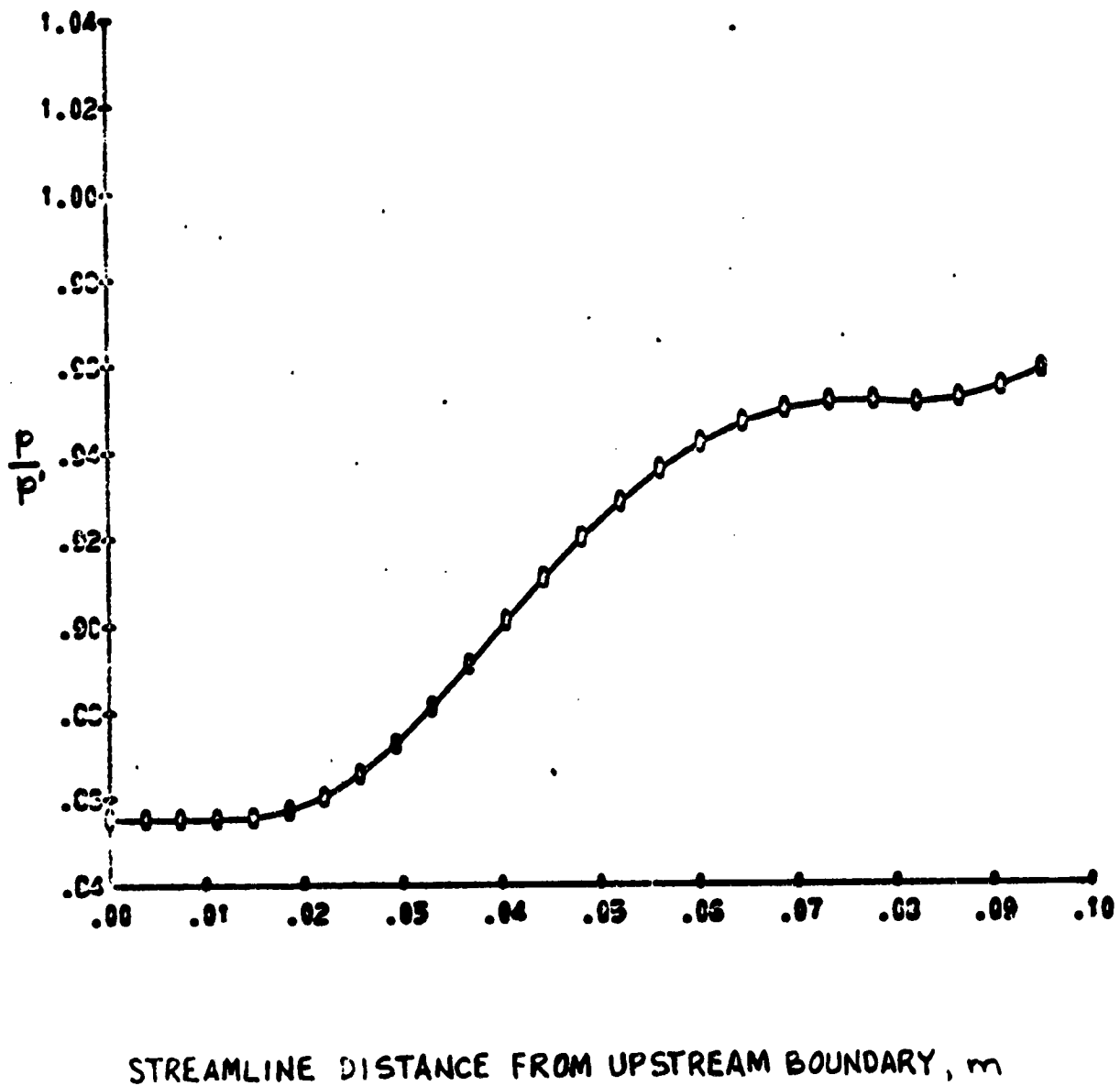
Figure 11. -- Continued
c. Design Point Static Pressure Distribution - Hub

STREAMLINE DISTANCE FROM UPSTREAM BOUNDARY , m.

Figure 11. -- Continued
d. Design Point Static Pressure Distribution - Shroud

Figure 11. -- Continued
e. 50% Gas Generator Speed Velocity Distribution - Hub

Figure 11. -- Continued
f. 50% Gas Generator Speed Velocity Distribution - Shroud

Figure 11. -- Continued
e. 50% Gas Generator Speed Velocity Distribution - Hub

Figure 11. -- Continued
    f. 50% Gas Generator Speed Velocity Distribution - Shroud

Figure 11. -- Continued
e. 50% Gas Generator Speed Velocity Distribution - Hub

Figure 11. -- Continued
f.   50% Gas Generator Speed Velocity Distribution - Shroud

STREAMLINE DISTANCE FROM UPSTREAM BOUNDARY, m

Figure 11. -- Continued
   g.   50% Gas Generator Speed Static Pressure Distribution - Hub

STREAMLINE DISTANCE FROM UPSTREAM BOUNDARY, m

Figure II. -- Concluded
    h.   50% Gas Generator Speed Static Pressure Distribution - Shroud

Figure 12 - [...] At stator leading edge.

Figure 13.- Diffuser duct. See Table X.
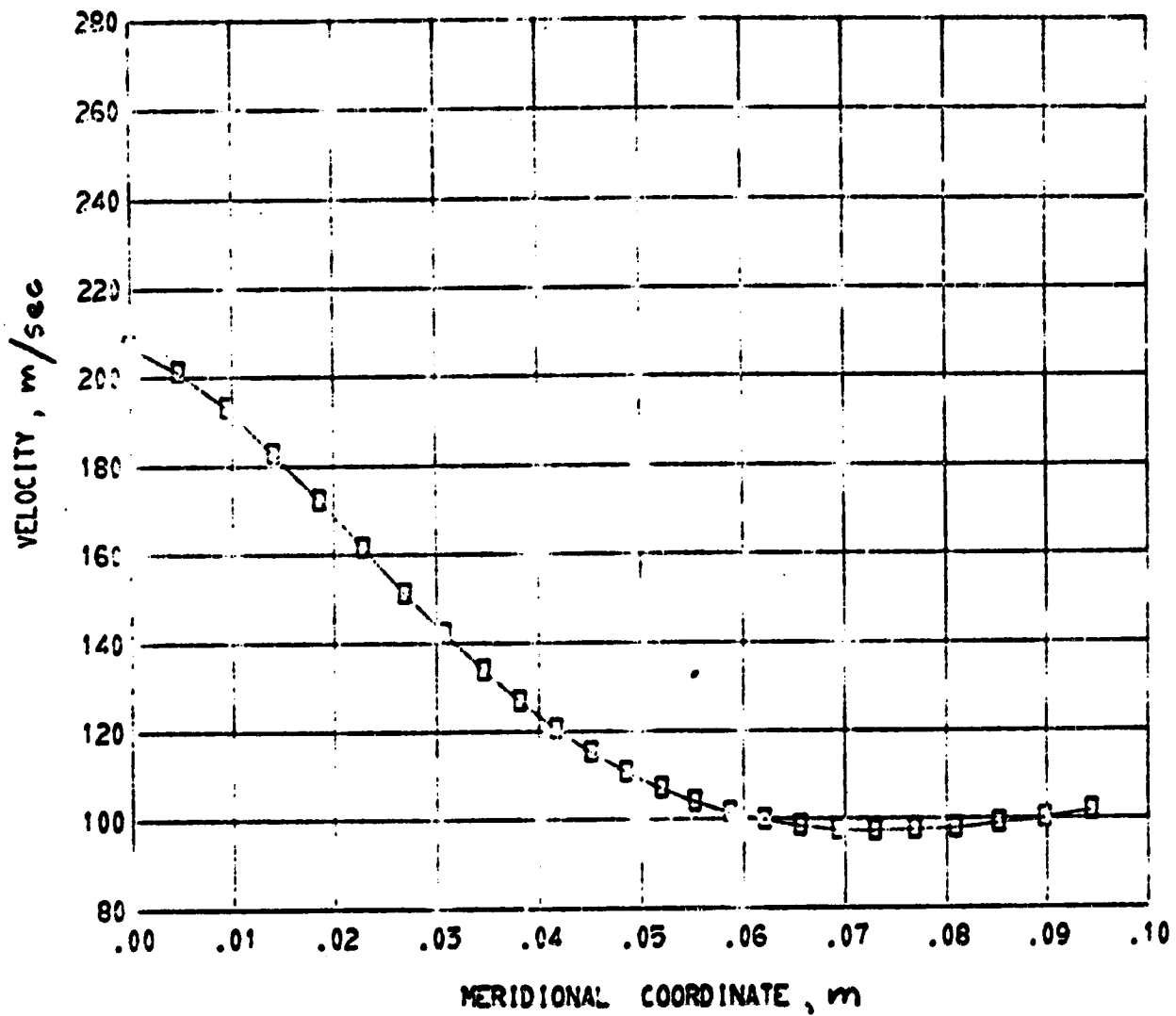
Figure 14. -- Diffuser Duct
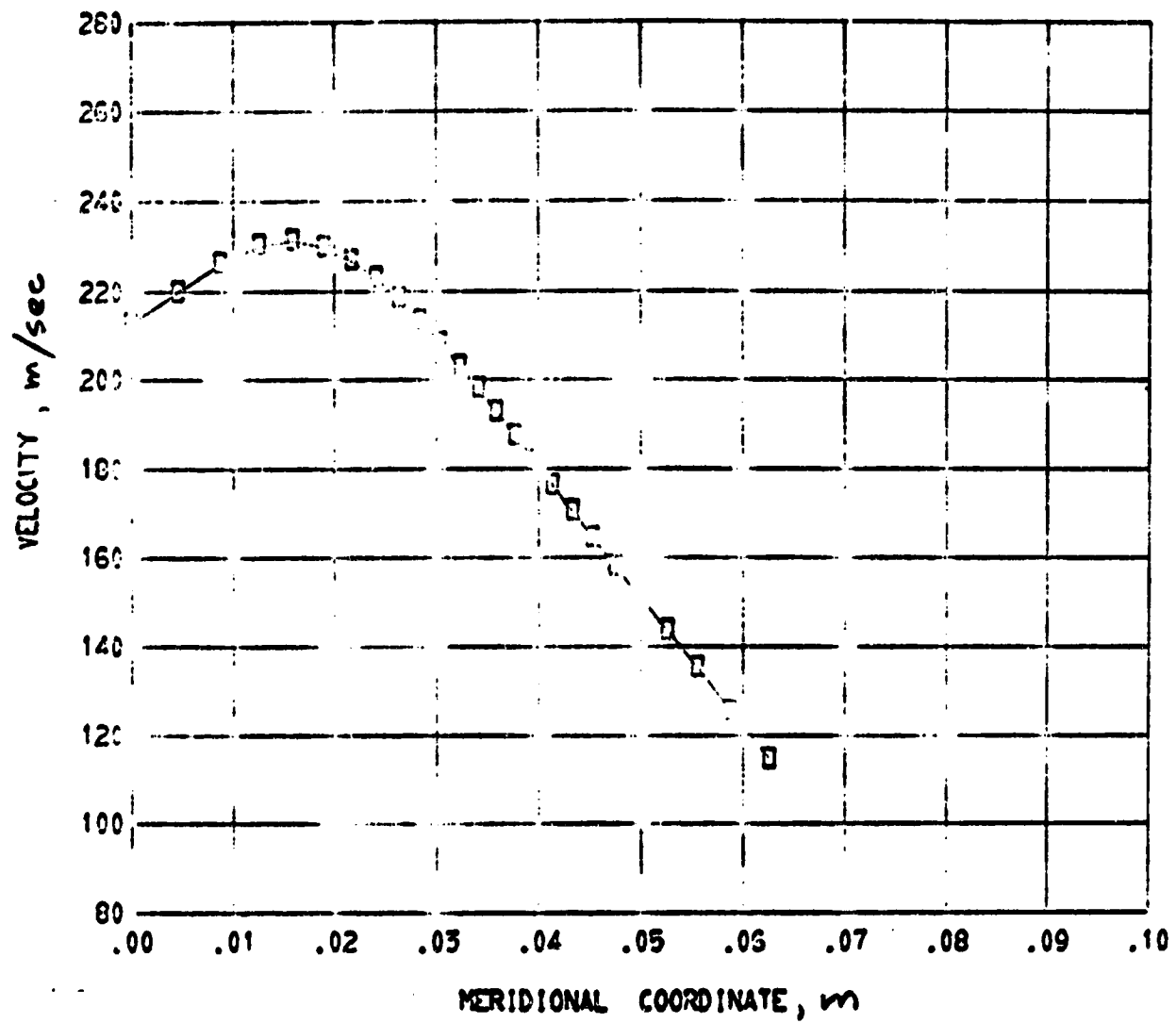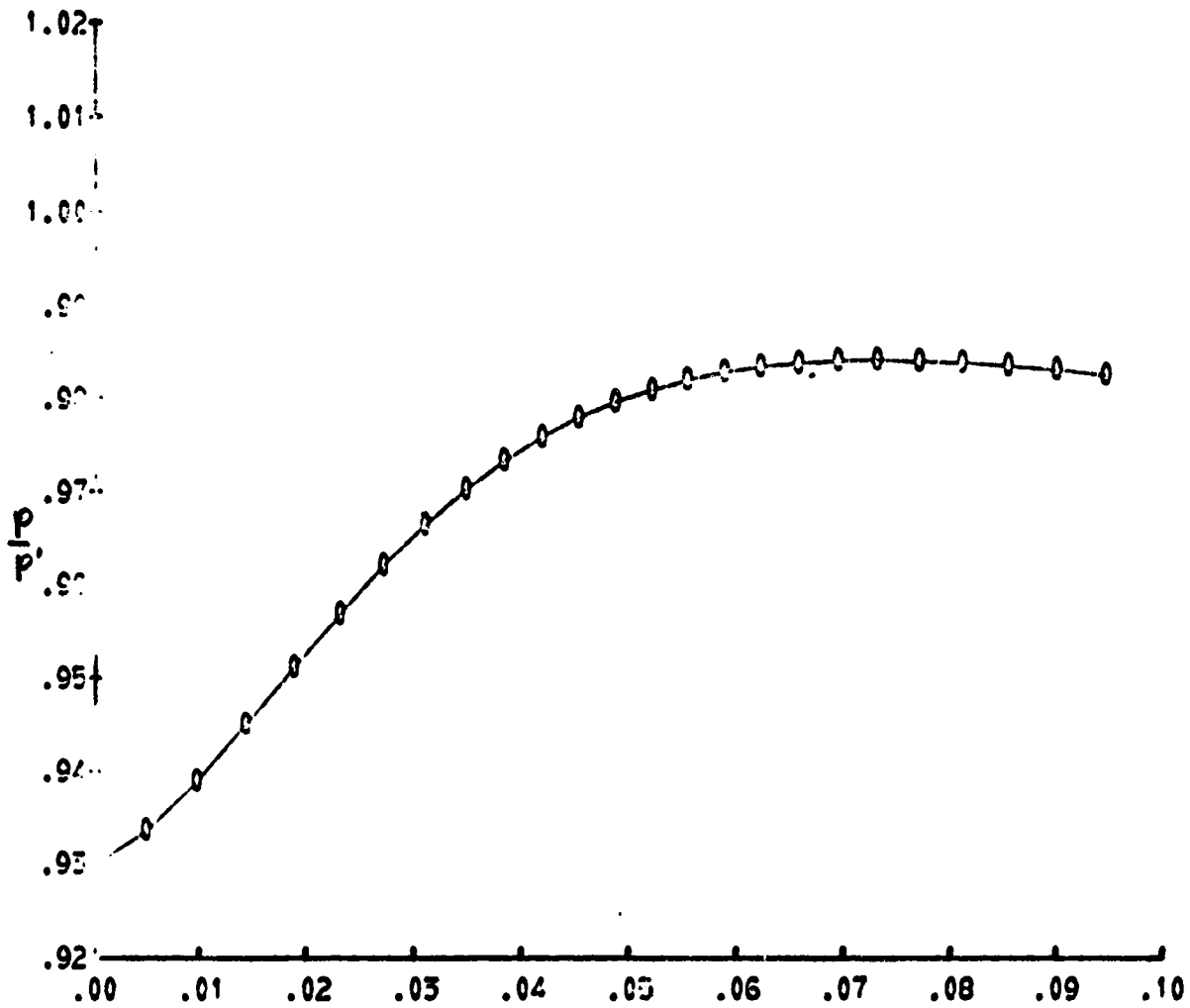a. Design Point Velocity Distribution - Hub

Figure 14. -- Continued
   b. Design Point Velocity Distribution - Shroud

STREAMLINE DISTANCE FROM UPSTREAM BOUNDARY, m

Figure 14. -- Continued
c.   Design Point Static Pressure Distribution - Hub

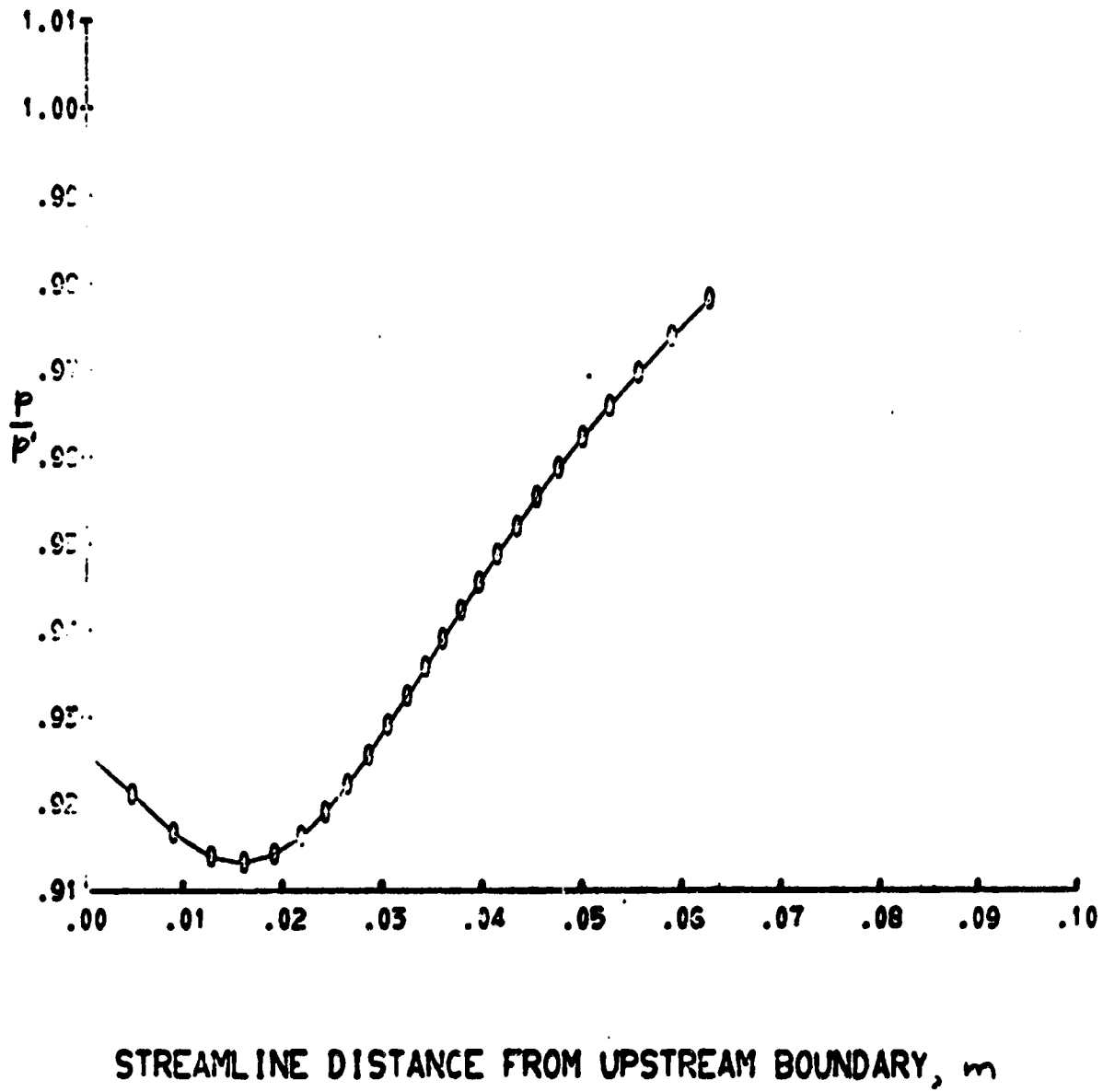STREAMLINE DISTANCE FROM UPSTREAM BOUNDARY, m

Figure 14. -- Concluded
    d. Design Point Static Pressure Distribution - Shroud